

RESEARCH PAPER

## Barium Oxide nanoparticles with Robust Catalytic, Photocatalytic and Humidity Sensing Properties

R. Renukadevi<sup>1</sup>, R. Sundaram<sup>1\*</sup> and K. Kaviyarasu<sup>2,3</sup>

<sup>1</sup> Department of Chemistry, Presidency College (Autonomous), Chennai - 600005, India.

<sup>2</sup> UNESCO-UNISA Africa Chair in Nanoscience's/Nanotechnology Laboratories, College of Graduate Studies, University of South Africa (UNISA), Muckleneuk Ridge, P O Box 392, Pretoria, South Africa.

<sup>3</sup> Nanoscience's African network (NANOAFNET), Materials Research Group (MRG), iThemba LABS-National Research Foundation (NRF), 1 Old Faure Road, 7129, P O Box 722, Somerset West, Western Cape Province, South Africa.

### ARTICLE INFO

#### Article History:

Received 20 August 2019

Accepted 16 October 2019

Published 01 January 2020

#### Keywords:

Barium Oxide

Epoxidation

Humidity Sensor

Photocatalyst

Rhodamine-B

### ABSTRACT

Barium Oxide (BaO) nanoparticles were synthesized by simple co-precipitation method and were investigated by the catalytic activity of synthesized barium oxide nanoparticles was enumerated by epoxidation of styrene. The reaction was carried out and the product was obtained at higher efficiency. Particularly, the photocatalytic efficiency was estimated by degradation of Rhodamine-B (RhB) dye using barium oxide nanoparticles under visible light illumination. The degraded dye concentration decreases nearly to zero at 60 minutes of its contact with photocatalyst. The humidity sensing properties of the material was measured by using DC resistance measurement at room temperature that reveals the sensitivity factor of 1926. Barium oxide nanoparticles shows the response and recovery characteristics of 40s and 110s respectively. The dye started to degrade and the concentration of the dye decreases to almost zero at 1 hour of irradiation that was predicted from the degradation rate which was the plot of C/C<sub>0</sub>. The degradation efficiency was found to be 98% for 1 hour degradation. The evaluation outline on performance basis revealed that synthesized barium oxide acts as a promising catalyst, photocatalyst and humidity sensing material were reported in detail.

#### How to cite this article

Renukadevi R, Sundaram R, Kaviyarasu K. Barium Oxide nanoparticles with Robust Catalytic, Photocatalytic and Humidity Sensing Properties. J Nanostruct, 2020; 10(1): 167-176. DOI: 10.22052/JNS.2020.01.018

### INTRODUCTION

Nanoscience and nanotechnology finds eminent place in scientific research due to its enormous applications which relies on its design and size [1]. Nanoparticles possesses significant properties such as physical, chemical, electronic, mechanical, medicinal, biological, catalytic, optical, magnetic properties due to which they find application in numerous areas [2-4]. There were various methods for the synthesis of nanoparticles such as Precipitation [5], sonochemical [5], solid

state [5], sol-gel [6], microwave [6], hydrothermal [7, 8], supersaturated reverse micelles and microemulsion method [9]. On the development of nanospecies - metal oxides holds a distinct place because of its wide range of properties due to which it finds numerous applications [10]. Specifically, semiconductor nanomaterials possess desirable applications in catalyst, sensors, photoelectron, highly functional and effective devices [11]. Among various metal oxides, specifically, barium

\* Corresponding Author Email: [drsundarampresidency@gmail.com](mailto:drsundarampresidency@gmail.com)

oxide holds unique place due to its wide bandgap. Epoxides are important intermediates in fine chemicals and pharmaceuticals synthesis. The conventional catalyst for the epoxidation was seemed to be unsafe, corrosive and expensive. Among alkaline, rare earth metal oxides - barium oxide possesses high catalytic activity towards epoxidation of terminal alkenes such as styrene [12]. Barium oxide or other alkaline earth metal oxides facilitate reforming other catalyst [13].

Photocatalyst produces electron-hole pairs upon the absorption of light quanta they react chemically with substrates that come into contact with them [14]. A dye seems to be major contributor to various pollution, which are difficult to decompose as they cause a variety of health issues to living systems. Rhodamine-B, a widely used dye, acts as organic pollutant and had been attracting the research interest since the past decades. Rhodamine B degradation occurs mainly through the photocatalytic process [15]. Humidity measurements are of great importance in many areas such as meteorology, medicine, industries, agriculture, warehousing, goods maintenance, preservation and manufacturing process control etc [16, 17]. Humidity sensors were based on the principle of adsorption of water molecule on the surface. The electrical properties changes by water adsorption on ceramic surfaces which encompasses the resistance, capacitance, electrolytic conduction depending upon the sensor type [18]. Based on the properties of barium oxide nanoparticles, hereby we investigate the catalytic, photocatalytic and humidity sensing ability. The novelty of the research work lies with the synthesis of BaO nanoparticle with varied applications. The BaO with diversified applications of catalytic, photocatalytic and RH humidity sensing properties were consolidated in this research work.

## MATERIALS & METHODS

Barium oxide nanoparticles were synthesized by simple co-precipitation technique [19]. Initially 0.1M solution of barium chloride and 0.1M solution of potassium hydroxide was prepared using de-ionised water. The solutions were added together slowly with continuous stirring and the mixture was magnetically stirred further for 45 minutes at room temperature. The resulting white precipitate was filtered and dried. The structural information and crystallography of the sample was analyzed by powder XRD. The diffraction patterns

were recorded with diffractometer system "XPRT - PRO" using (copper-anode material)  $\text{CuK}\alpha$  ( $\lambda=1.5406$  nm) at room temperature. The mean particle size and morphology of the sample were characterized by scanning electron microscope using AU Quanta 250FEG at 10KV with different range of magnification and transmission electron microscopy (JEM 2100F). The purity of the sample was examined by EDX using detector type SDD APOLLO X. Optical properties of the synthesized metal oxide was examined using UV-visible spectrophotometer JASCO V-630. The epoxidation reaction of styrene over the catalyst was carried out using 0.1 g of barium oxide nanoparticles as catalyst with 10 mmol of styrene and 15 mmol of TBHP under reflux at 85 °C and the reaction mixture was vigorously stirred under reflux [20]. TLC for the reaction was carried out in regular interval of time that indicates the completion of the reaction. The photocatalytic ability was examined by the photodegradation of Rhodamine-B using synthesized photocatalyst under visible-light irradiated by a 250 W tungsten-halogen lamp as a light source [21]. For the photodegradation of dye, 100 mL of the aqueous RhB ( $2 \times 10^{-5}$  M) solution was taken with 25 mg of barium oxide nanoparticles.

Before irradiation, the suspensions were magnetically stirred in dark for 30 min for reaching equilibrium between the dye and photo-catalyst. At regular time intervals, 3 mL of the suspension were collected and centrifuged for further analysis by UV-studies. The concentration of RhB was measured using a UV - visible spectrophotometer JASCO V-630 instrument. DC measurements of the synthesized material were carried out using a two-probe method. Anhydrous  $\text{P}_2\text{O}_5$  and saturated aqueous solutions of  $[\text{CH}_3\text{COOK}]$ ,  $[\text{CaCl}_2 \cdot 6\text{H}_2\text{O}]$ ,  $[\text{Zn}(\text{NO}_3)_2 \cdot 6\text{H}_2\text{O}]$ ,  $[\text{Ca}(\text{NO}_3)_2 \cdot 4\text{H}_2\text{O}]$ ,  $[\text{NaNO}_2]$ ,  $[\text{NH}_4\text{Cl}]$ ,  $[\text{BaCl}_2 \cdot 2\text{H}_2\text{O}]$  and  $[\text{CuSO}_4 \cdot 5\text{H}_2\text{O}]$  in a closed glass vessel at room temperature were used for controlled humidity environments which yielded 5, 20, 31, 42, 51, 66, 79, 88 and 98 % relative humidity (RH) respectively which were monitored by using a barigo hygrometer. The samples were placed in each humidity buffers for water adsorption on the surface for 2 hours. The resistivities of the composites were determined under each humidity buffer atmosphere by using Agronic -53C model digital micro ohm meter. The response and recovery time of the sensing material were also evaluated [16].

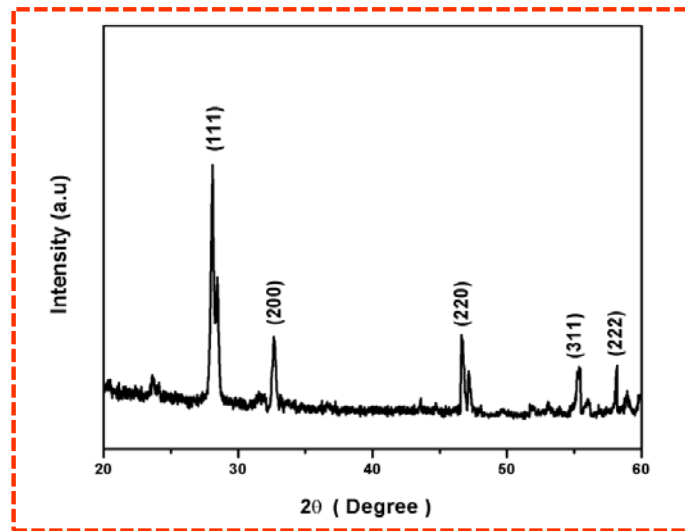


Fig. 1. Powder X-ray diffraction pattern of barium oxide nanoparticles.

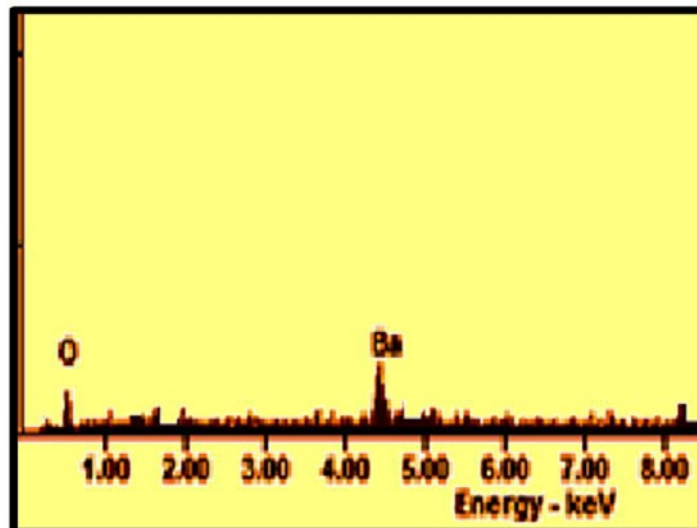


Fig. 2. EDX spectrum of barium oxide nanoparticles.

## RESULTS AND DISCUSSION

The XRD pattern of as prepared barium oxide nanoparticles as shown in Fig. 1. It exhibits cubic system with face centered lattice structure as obtained in [JCPDS File No.74-1228]. Phase characterization by powder XRD of the samples give a sharp diffraction peaks. The XRD peaks indexed coincides with standard peaks corresponding to  $(hkl)$  values of (111), (200), (220), (311), (222) which indicates that the prepared material has no impurity phases. The crystallite size of the synthesized BaO nanoparticles was calculated using the scherrer formula [22],

$$D = k\lambda / \beta \cos\theta$$

Where  $D$  = crystallite size,  $k=0.9$ ,  $\lambda$  = wavelength of the incident light,  $\theta$  = angle of diffraction and  $B$  = full width half maxima on  $2\theta$  scale. The calculated crystallite size of the synthesized BaO nanoparticles ranges between 11 nm and 41 nm. The average crystallite size of the BaO nanoparticles under investigation was found to be 28 nm. The EDX spectrum of the sample as shown in Fig. 2. It shows the presence of elements barium and oxygen which his implies that the synthesized

barium oxide nanoparticles contains no impurity. SEM shown in Fig. 3(a) analyzed the shape and morphology of the material which clearly exhibits irregular arrangement of nearly spherical shapes with pores that facilitate easier adsorption and desorption. The agglomeration of the particles in the image may be due to influence of interfacial energy. TEM analysis was further carried out for the morphology and crystal structure of BaO nanoparticles. Fig. 3(b) shown the TEM images is an individual and complete nanoparticles. Fig. 3(c) shows the particle size of the barium oxide nanoparticles. The particle size averages around 32 nm which was nearly around the calculated size from XRD pattern. The high intensity exhibits that most of the synthesized particles were around 32 nm in size. A very few particles shows growth in size that were ranged around 120 nm. However, the size of the synthesized nanoparticles were not uniform which may be due to the synthesis

procedure. The light absorption properties were investigated by UV absorption spectra of BaO nanoparticles given in Fig. 4. It could be observed that the absorption edge was at 325 nm. The bandgap energy  $E_g$  values was calculated based on the formula  $E_g = 1240/\lambda$ , where the  $\lambda$  is the absorption edge [23] and the calculated band energy gap value was 3.82 eV. The wide bandgap facilitates better performance of the material. The catalytic performance of barium oxide nanoparticles was examined through epoxidation of styrene. The product formation was monitored by TLC. It produces yield at 1h and the percentage yield was found to be 82% which was good when compared to conventional methods [12]. The catalyst was separated from the reaction mixture by filtration. The catalyst amount was varied to understand the effect of catalyst on the reaction. The reaction was repeated with change in the amount of catalyst with all other conditions similar

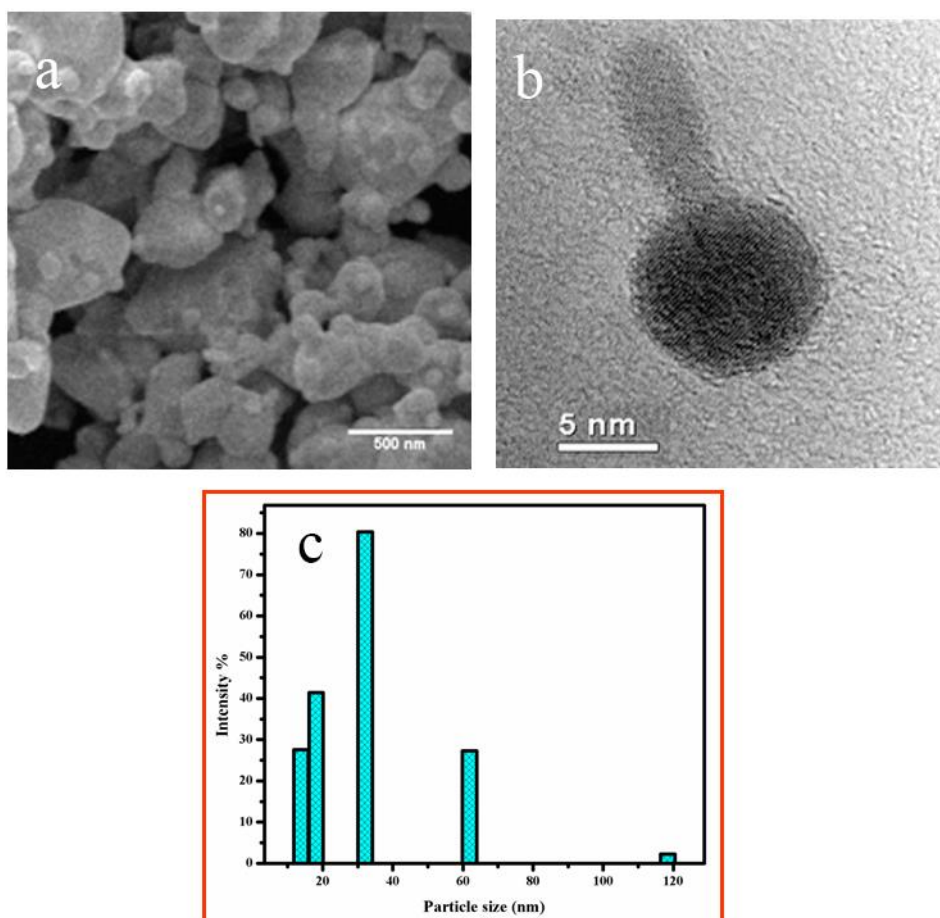


Fig. 3(a). SEM image of the barium oxide nanoparticles (b) TEM image of the barium oxide nanoparticles (c) Particle size of the barium oxide nanoparticles.

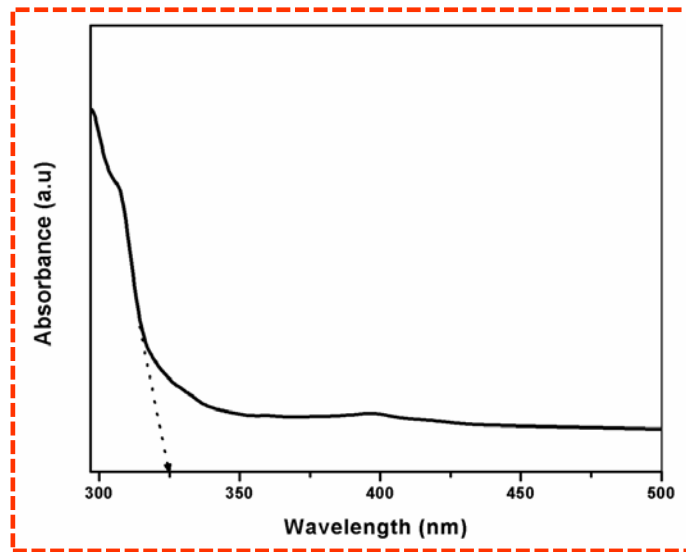


Fig. 4. UV absorption spectra of barium oxide nanoparticles.

[24]. The obtained results of catalytic activity were given in Fig. 5. It predicts that when the amount of catalyst is doubled/tripled there was no rapid or major change in yield/product formed. Thus, 0.1g of catalyst was assumed as the saturated level. The photocatalytic activity of the synthesized barium oxide nanoparticles was assessed for the photodegradation of Rhodamine-B under visible-light illumination. The photolysis of Rhodamine-B alone (blank) was performed without any

photocatalyst under visible-light illumination. It is revealed that there was no considerable Rhodamine-B photodegradation was observed even for 90 min of light illumination.

The photodegradation of Rhodamine-B by BaO nanomaterial were evaluated under visible-light illumination and the results are shown in Fig. 6. The dye started to degrade and the concentration of the dye decreases to almost zero at 1hour of irradiation that was predicted from

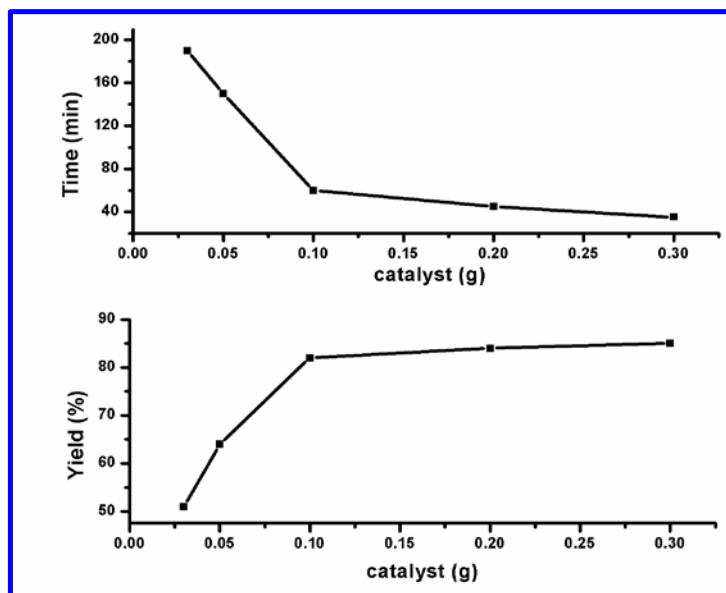


Fig. 5. Catalytic efficiency of the barium oxide nanoparticles.

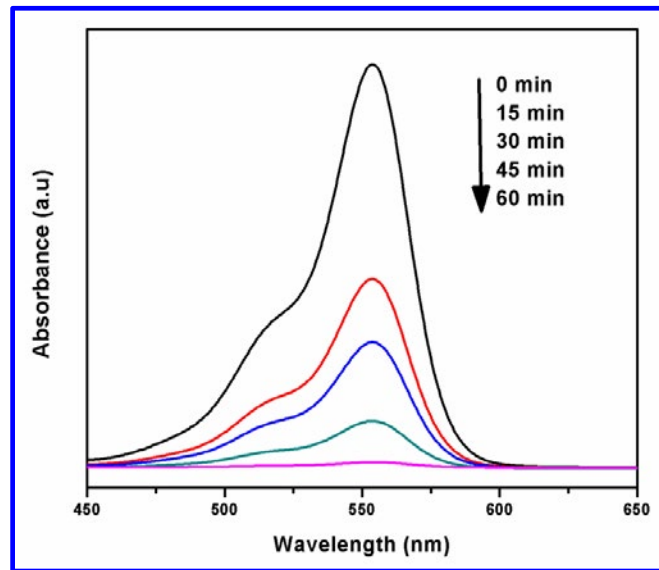


Fig. 6. Photocatalytic degradation of RhodamineB in barium oxide nanoparticles.

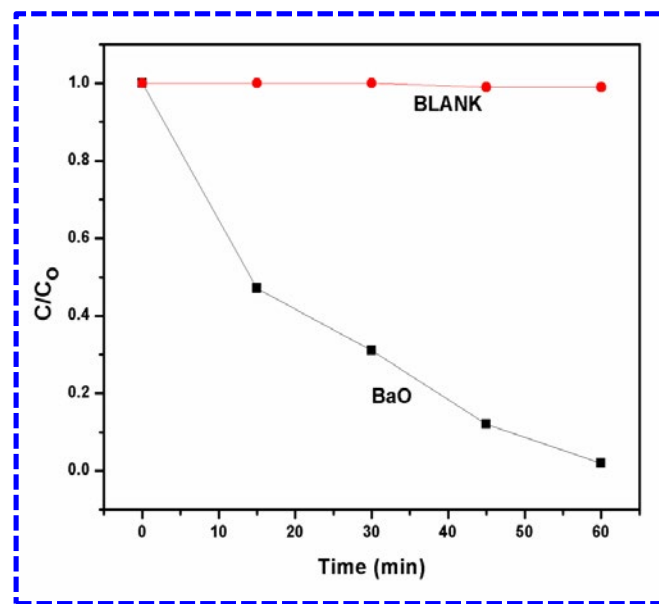
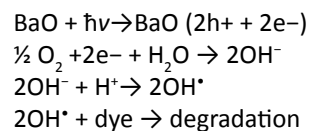


Fig. 7. Degradation diagram of Rhodamine B with and without photocatalyst barium oxide nanoparticles.

the degradation rate [25] which was the plot of  $C/C_0$  given in Fig. 7. The degradation efficiency was found to be 98% for 1hour degradation. The plot for blank was a straight line whereas the line for the photocatalyst material is a linear slope. This was an additional evidence for the better performance of the photocatalyst. The mechanism [26] of photocatalysis was given in Fig. 8. which was explained below;



Where ' $h$ ' is Planck's constant and ' $\nu$ ' is the frequency of visible light. The reaction by the synthesized BaO nanoparticles produce radicals that facilitates the degradation of RhB. The OH

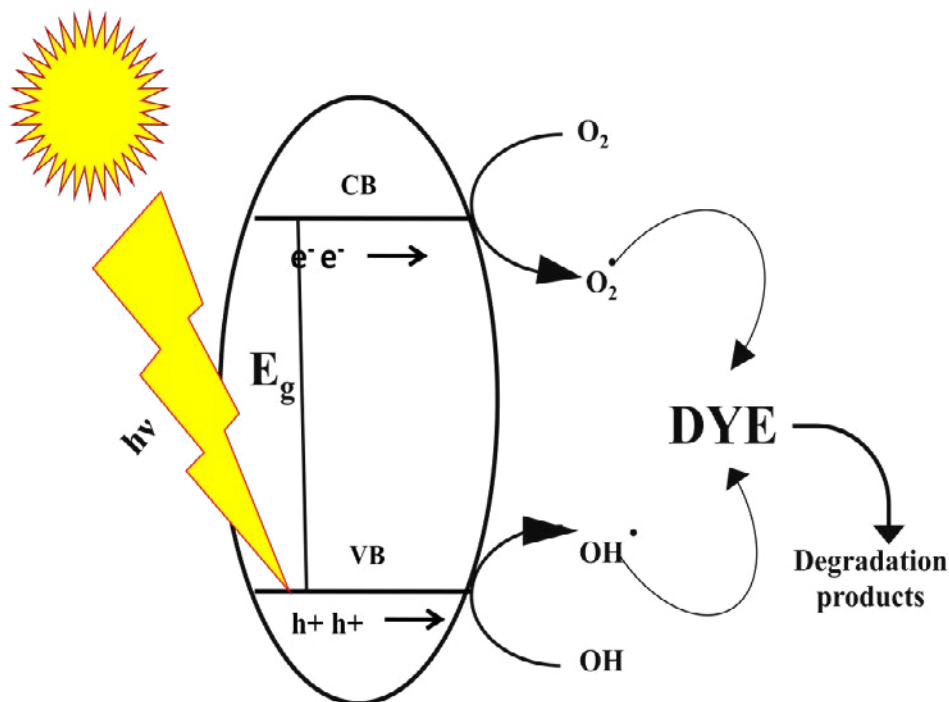


Fig. 8. Photocatalytic degradation mechanism of barium oxide nanoparticles.

group was converted into its radical form which degrades the dye [27]. Similarly the oxygen super oxide anions are produced by BaO upon irradiation. The produced oxygen super oxide anions facilitate degradation of Rh B [28]. The barium oxide nanoparticles were placed in different humidity buffers ranging from 5% to 98% RH. The resistance of the material at each humidity buffers was calculated. The sensitivity factor ( $S_f$ ) was calculated from the ratio  $R_{5\%}/R_{98\%}$ , where  $R_{5\%}$  and  $R_{98\%}$  are the DC resistances at 5% and 98 % RH respectively. A good humidity sensor material possesses high sensitivity factor ( $S_f = R_{5\%} / R_{98\%}$ ) and the linear plot of  $\log R$  vs. RH (%). The sensitivity factor ( $S_f$ ) value of the synthesized nanoparticle was 1926. The plot of  $\log R$  vs. RH (%) which was given in Fig. 9. That explains sensitivity towards moisture. As the humidity is increased, the  $\log R$  values drops. The significant feature is in the plot of  $\log R$  with RH (%) which is almost linear. The sensitivity factor of should be indicative of the extent of moisture condensation in the pores. The humidity sensors of this type follows the mechanism of the adsorption of water molecules.

Water molecules gets adsorbed on the oxide surface following electronic path of mechanism

that was due to quick adsorption between water molecules and adsorbed oxygen species followed by desorption of the adsorbed oxygen species [29]. The adsorption involving physisorption at the surface of the synthesized nanoparticles by the water molecules plays vital role which alters the electrical measurements/readings (resistance). When the humidity increases, the adsorption increases and thus the resistance drops simultaneously. The response and recovery time are important characteristics for a commercial type of humidity sensor. The time response of a sensor can vary from sensor to sensor by seconds to hours. The response of sensing material can be calculated by allowing humidity in the chamber from 5% RH to 98% RH and for calculating the recovery time of sensing material humidity in chamber was reduced from 98% RH to 5% RH. The response and recovery plot were given in Fig. 10. It enumerates the quick responding and recovering sensing ability of the synthesized material. The response of the sensing material was 40s and the recovery time of the sensing material was 110s that was seemed to be quietly prominent time and thus the barium oxide nanoparticles exhibits excellent humidity sensing behavior.

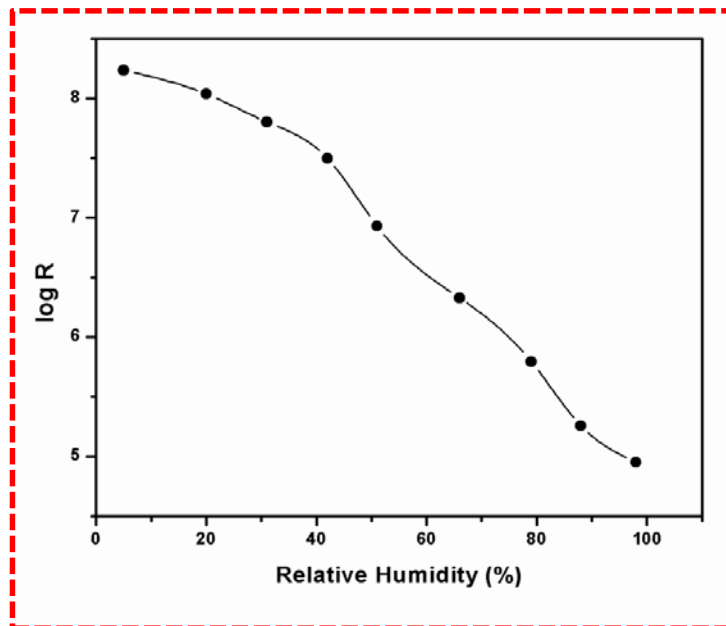


Fig. 9. Relative humidity (RH) % vs log R studies of barium oxide nanoparticles.

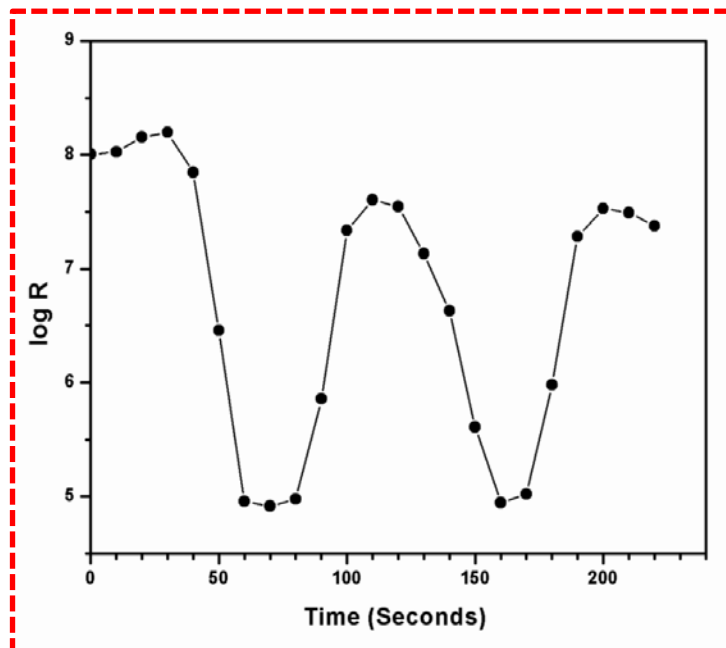


Fig. 10. Response and recovery time measurement studies of barium oxide nanoparticles.

### CONCLUSION

Nanosized barium oxide particles were successfully synthesized which was in accordance with [JCPDS Card No. 74-1228] that was pure, nearly spherical particles with bandgap of 3.8eV.

The epoxidation of styrene was seemed to possess better efficiency of 82%. The photocatalytic degradation of organic pollutants-dyes particularly Rhodamine-B was at higher rate of 98%. The humidity sensing property of the synthesized

barium oxide was satisfactory with  $S_f$  value of 1926. The response time was 40s and the recovery time was 110s. The synthesized barium oxide nanoparticle is of great importance because of its wide properties thus facilitating its applications in numerous areas.

#### ACKNOWLEDGEMENT

The authors are thankful to Director of Collogiate Education, Tamil Nadu Government Higher Education and Government of Tamilnadu for funding scholarship for the scholar to carryout the research work with Reference to 49500/K2/2015.

#### CONFLICT OF INTEREST

The authors declare that there is no conflict of interests regarding the publication of this manuscript.

#### REFERENCES

- Ganguli AK, Ganguly A, Vaidya S. Microemulsion-based synthesis of nanocrystalline materials. *Chem Soc Rev*. 2010;39(2):474-85.
- Renukadevi R, Sundaram R. Facile Synthesis of Zinc Oxide Nanoparticles with Antibacterial, Humidity Sensing and Photocatalytic Behaviour. *International Journal of Research in Advent Technology*. 2019;7(1):432-9.
- Kaviyarasu K, Sajan D, Selvakumar MS, Augustine Thomas S, Prem Anand D. A facile hydrothermal route to synthesize novel PbI<sub>2</sub> nanorods. *Journal of Physics and Chemistry of Solids*. 2012;73(11):1396-400.
- Kaviyarasu K, Manikandan E, Kennedy J, Jayachandran M. Quantum confinement and photoluminescence of well-aligned CdO nanofibers by a solvothermal route. *Materials Letters*. 2014;120:243-5.
- Ghiyasiyan-Arani M, Salavati-Niasari M. Effect of Li<sub>2</sub>CoMn<sub>3</sub>O<sub>8</sub> Nanostructures Synthesized by a Combustion Method on Montmorillonite K10 as a Potential Hydrogen Storage Material. *The Journal of Physical Chemistry C*. 2018;122(29):16498-509.
- Salehabadi A, Sarrami F, Salavati-Niasari M, Gholami T, Spagnoli D, Karton A. Dy<sub>3</sub>Al<sub>2</sub>(AlO<sub>4</sub>)<sub>3</sub> ceramic nanogarnets: Sol-gel auto-combustion synthesis, characterization and joint experimental and computational structural analysis for electrochemical hydrogen storage performances. *Journal of Alloys and Compounds*. 2018;744:574-82.
- Mazloom F, Ghiyasiyan-Arani M, Monsef R, Salavati-Niasari M. Photocatalytic degradation of diverse organic dyes by sol-gel synthesized Cd<sub>2</sub>V<sub>2</sub>O<sub>7</sub> nanostructures. *Journal of Materials Science: Materials in Electronics*. 2018;29(21):18120-7.
- Monsef R, Ghiyasiyan-Arani M, Salavati-Niasari M. Utilizing of neodymium vanadate nanoparticles as an efficient catalyst to boost the photocatalytic water purification. *Journal of Environmental Management*. 2019;230:266-81.
- Safardoust-Hojaghan H, Shakouri-Arani M, Salavati-Niasari M. A facile and reliable route to prepare of lead sulfate nanostructures in the presence of a new sulfur source. *Journal of Materials Science: Materials in Electronics*. 2014;26(3):1518-24.
- Ramimoghdam D, Bin Hussein MZ, Taufiq-Yap YH. Hydrothermal synthesis of zinc oxide nanoparticles using rice as soft biotemplate. *Chemistry Central Journal*. 2013;7(1).
- H. Bari R, B. Patil S, Bari AR. SYNTHESIS, CHARACTERIZATION AND GAS SENSING PERFORMANCE OF SOL-GEL PREPARED NANOCRYSTALLINE SnO<sub>2</sub> THIN FILMS. *International Journal on Smart Sensing and Intelligent Systems*. 2014;7(2):610-29.
- Choudhary VR, Jha R, Jana P. Epoxidation of styrene by TBHP to styrene oxide using barium oxide as a highly active/selective and reusable solid catalyst. *Green Chemistry*. 2006;8(8):689.
- Yang L, Choi Y, Qin W, Chen H, Blinn K, Liu M, et al. Promotion of water-mediated carbon removal by nanostructured barium oxide/nickel interfaces in solid oxide fuel cells. *Nature Communications*. 2011;2(1).
- Jo W-K, Tayade RJ. Recent developments in photocatalytic dye degradation upon irradiation with energy-efficient light emitting diodes. *Chinese Journal of Catalysis*. 2014;35(11):1781-92.
- Fu H, Pan C, Yao W, Zhu Y. Visible-Light-Induced Degradation of Rhodamine B by Nanosized Bi<sub>2</sub>WO<sub>6</sub>. *The Journal of Physical Chemistry B*. 2005;109(47):22432-9.
- Renukadevi, R. Renukadevi R. and Rajyashree M. Sundaram. "Surfactant – free , facile synthesis of zinc tungstate nanoparticles for photocatalytic , antibacterial and humidity sensing applications." (2019).
- Zhang Y, Hou Y, Liu W, Zhang H, Zhang Y, Zhang Z, et al. A Cost-Effective Relative Humidity Sensor Based on Side Coupling Induction Technology. *Sensors*. 2017;17(5):944.
- Renukadevi R, Sundaram R. Synthesis, Characterization, Humidity Sensing, Antibacterial, Photocatalytic and Kinetic Studies of Novel HgWO<sub>4</sub> – WO<sub>3</sub> Nanocomposites. *Materials Today: Proceedings*. 2019;8:153-61.
- Suresh G, Nirmala PN. Synthesis of barium oxide nanorod by chemical bath deposition. *Turkish Journal of Physics*. 2012 25;36(3):392-397.
- Patil NS, Uphade BS, Jana P, Sonawane RS, Bhargava SK, Choudhary VR. Epoxidation of Styrene by Anhydrous t-Butyl Hydroperoxide over Au/TiO<sub>2</sub>Catalysts. *Catalysis Letters*. 2004;94(1/2):89-93.
- Becker J, Raghupathi KR, St. Pierre J, Zhao D, Koodali RT. Tuning of the Crystallite and Particle Sizes of ZnO Nanocrystalline Materials in Solvothermal Synthesis and Their Photocatalytic Activity for Dye Degradation. *The Journal of Physical Chemistry C*. 2011;115(28):13844-50.
- Hassanpour M, Salavati-Niasari M, Tafreshi SAH, Safardoust-Hojaghan H, Hassanpour F. Synthesis, characterization and antibacterial activities of Ni/ZnO nanocomposites using bis(salicylaldehyde) complex precursor. *Journal of Alloys and Compounds*. 2019;788:383-90.
- Khan SB, Faisal M, Rahman MM, Akhtar K, Asiri AM, Alamry KA. Sensitive chemi-sensor for environmental applications as marker of chloroform in aqueous solution. *Spectrochimica Acta Part A: Molecular and Biomolecular Spectroscopy*. 2013;106:231-5.
- Papal B, Nagaraju S, Veerabhadrarai P, Sujatha K, Kanvah S, Vijaya Kumar B, et al. Recyclable Bi<sub>2</sub>WO<sub>6</sub>-nanoparticle

- mediated one-pot multicomponent reactions in aqueous medium at room temperature. *RSC Adv.* 2014;4(97):54168-74.
25. Dirany N, Arab M, Leroux C, Villain S, Madigou V, Gavarri JR. Effect of WO<sub>3</sub> Nanoparticles Morphology on the Catalytic Properties. *Materials Today: Proceedings.* 2016;3(2):230-4.
26. Kaviyarasu K, Ayeshamariam A, Manikandan E, Kennedy J, Ladchumananandasivam R, Umbelino Gomes U, et al. Solution processing of CuSe quantum dots: Photocatalytic activity under RhB for UV and visible-light solar irradiation. *Materials Science and Engineering: B.* 2016;210:1-9.
27. Hassanpour M, Safardoust-Hojaghan H, Salavati-Niasari M. Degradation of methylene blue and Rhodamine B as water pollutants via green synthesized Co<sub>3</sub>O<sub>4</sub>/ZnO nanocomposite. *Journal of Molecular Liquids.* 2017;229:293-9.
28. Hassanpour M, Salavati-Niasari M, Mousavi SA, Safardoust-Hojaghan H, Hamadian M. CeO<sub>2</sub>/ZnO ceramic nanocomposites, synthesized via microwave method and used for decolorization of dye. *Journal of Nanostructures.* 2018 Jan 1;8(1):97-106.
29. Chen Z, Lu C. Humidity Sensors: A Review of Materials and Mechanisms. *Sensor Letters.* 2005;3(4):274-95.